

# Single Low-Dose Nanovaccine for Long-Term Protection against Anthrax Toxins

Maya Holay, Nishta Krishnan, Jiarong Zhou, Yaou Duan, Zhongyuan Guo, Weiwei Gao, Ronnie H. Fang,\* and Liangfang Zhang\*



Cite This: <https://doi.org/10.1021/acs.nanolett.2c03881>



Read Online

ACCESS |

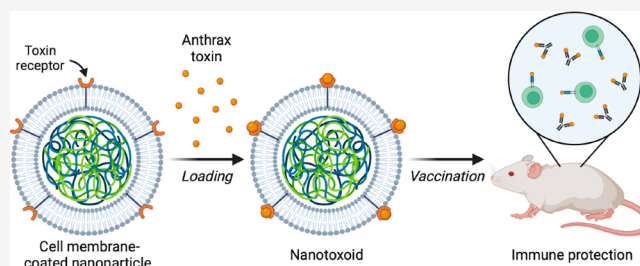
Metrics & More

Article Recommendations

Supporting Information

**ABSTRACT:** Anthrax infections caused by *Bacillus anthracis* are an ongoing bioterrorism and livestock threat worldwide. Current approaches for management, including extended passive antibody transfusion, antibiotics, and prophylactic vaccination, are often cumbersome and associated with low patient compliance. Here, we report on the development of an adjuvanted nanotoxoid vaccine based on macrophage membrane-coated nanoparticles bound with anthrax toxins. This design leverages the natural binding interaction of protective antigen, a key anthrax toxin, with macrophages. In a murine model, a single low-dose vaccination with the nanotoxoids generates long-lasting immunity that protects against subsequent challenge with anthrax toxins. Overall, this work provides a new approach to address the ongoing threat of anthrax outbreaks and bioterrorism by taking advantage of an emerging biomimetic nanotechnology.

**KEYWORDS:** anthrax, nanotoxoid, biomimetic nanoparticle, cell membrane coating, antivirulence vaccine



**B** *acillus anthracis*, the causative agent of anthrax, is a Gram-positive, spore-forming bacterium with a history of deadly outbreaks.<sup>1</sup> Today, anthrax is considered to be a highly potent bioterrorism agent and an ongoing threat to livestock populations worldwide.<sup>2</sup> *B. anthracis* spores can remain in the soil for decades, and they are resistant to many disinfectants and heat treatment.<sup>3</sup> As a result, the bacterium is incredibly difficult to eradicate. Spores can access the body through cutaneous, gastrointestinal, inhalational, and even injectable routes. Once germinated, the bacterium begins to replicate and produce highly lethal virulence factors. Some therapeutic approaches have been developed to combat anthrax, including the use of monoclonal antibodies (obitoximab) and antibiotics (ciprofloxacin and doxycycline).<sup>4</sup> However, due to the extended spore survival time in the body of up to 60 days, these therapies require long treatment regimens that have had historically low compliance rates.<sup>5,6</sup>

Lethal toxin, one of the primary virulence factors generated during an anthrax infection, consists of two subunits.<sup>7</sup> Protective antigen (PA) can bind to the plasma membrane of cells such as macrophages that express the appropriate receptors, including capillary morphogenesis gene 2 (CMG2).<sup>8</sup> Upon being activated by proteases on the cell surface, PA oligomerizes and binds to the enzymatically active lethal factor (LF).<sup>9</sup> The subsequent uptake and translocation of LF into the cytosolic compartment results in the disruption of signaling pathways and ultimately cellular apoptosis. Given its critical role in potentiating the activity of lethal toxin, PA has been a

major target for vaccination.<sup>10</sup> BioThrax, an FDA-approved vaccine against *B. anthracis*, contains purified PA and an alum adjuvant. While effective, the vaccine currently requires an initial five doses over 18 months and an annual booster, making it ineffective for widespread use or time-sensitive situations.<sup>11</sup> In addition, alum has been associated with severe local reactions and a lack of stability with recombinant PA.<sup>12–14</sup> Anthrax vaccines utilizing alternative adjuvants, such as CpG oligodeoxynucleotides<sup>15–17</sup> and trimethyl chitosan,<sup>18,19</sup> have also been explored. Overall, there is an urgent need for a cost-effective anthrax vaccine that requires fewer doses and can be easily distributed.

Cell membrane-coated nanoparticles, consisting of a naturally derived cell membrane layer camouflaging a synthetic nanoparticle core, are endowed with the surface characteristics of their source cells.<sup>20–24</sup> Among their various applications, including drug delivery,<sup>25–27</sup> biodetoxification,<sup>28,29</sup> and immune modulation,<sup>30–32</sup> these biomimetic nanoparticles are capable of complexing with toxins or other antigenic material via natural receptor–ligand interactions,<sup>29,33–35</sup> thus generating nanotoxoids that can be safely delivered *in vivo* as a vaccine

**Received:** October 3, 2022

**Revised:** November 15, 2022

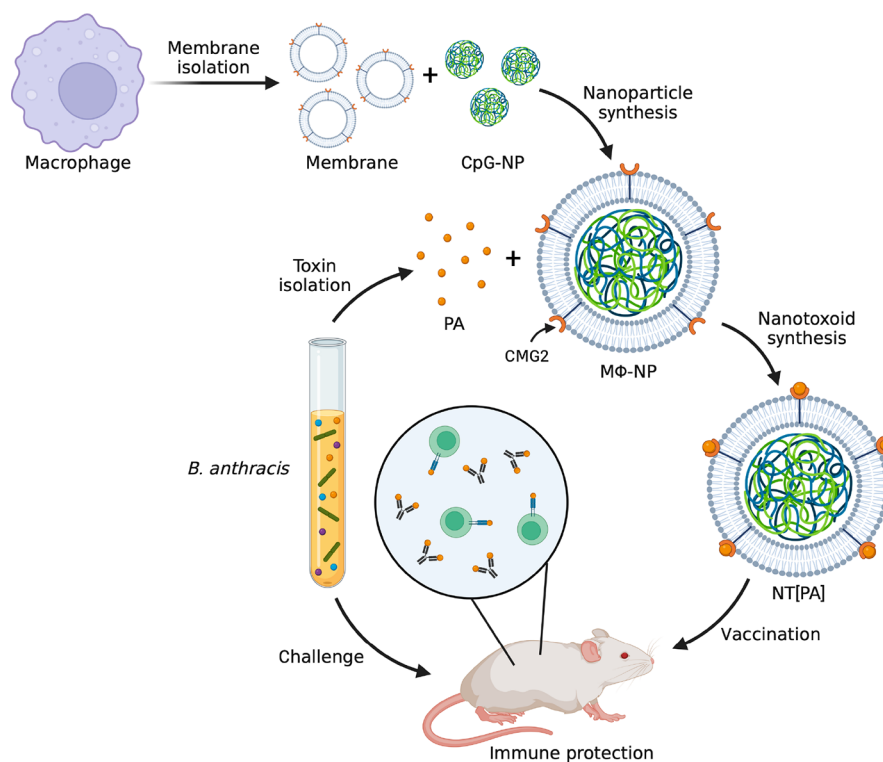


**Figure 1.** Nanotoxoids for protection against anthrax. Macrophage membrane-coated nanoparticles (MΦ-NPs) are fabricated by coating macrophage membrane expressing the anthrax receptor CMG2 onto polymeric CpG-loaded nanoparticle cores (CpG-NPs). MΦ-NPs are then complexed with anthrax toxin protective antigen (PA) to form nanotoxoids (NT[PA]). Mice vaccinated with NT[PA] generate antigen-specific immunity that protects them from anthrax toxins. Created with BioRender.

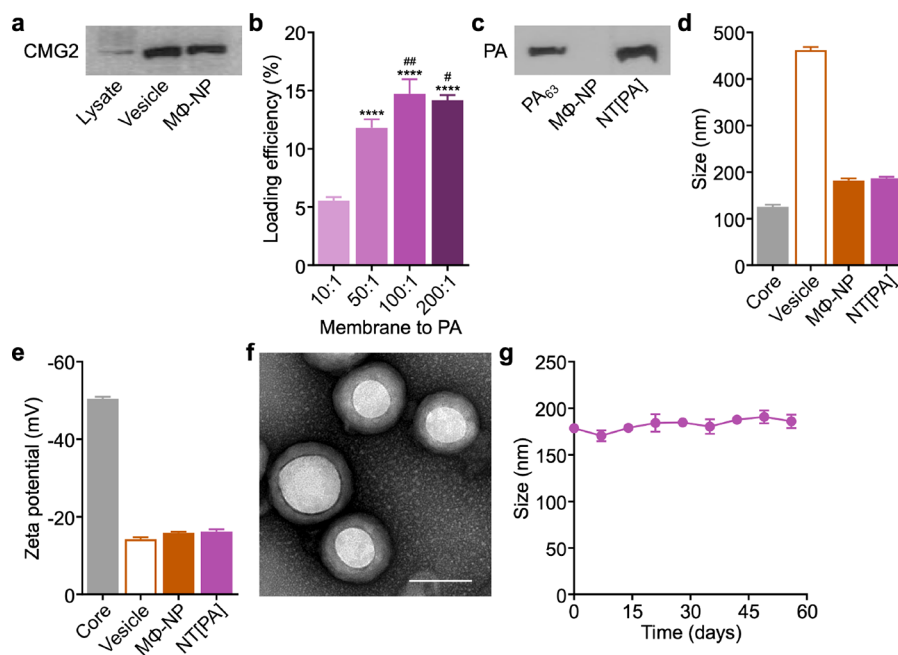


**Figure 2.** Nanoparticle fabrication and characterization. (a) Western blot for CMG2 expression in J774 whole cell lysate, J774 membrane vesicles, and MΦ-NPs. (b) PA loading efficiency onto MΦ-NPs at varying membrane protein to PA weight ratios ( $n = 3$ , mean + SD). \*\*\*\* $p < 0.0001$  (compared to 10:1); # $p < 0.05$ , ## $p < 0.01$  (compared to 50:1); one-way ANOVA. (c) Western blot for PA expression on MΦ-NPs and NT[PA]. (d, e) Hydrodynamic size (d) and zeta potential (e) of PLGA nanoparticle cores, J774 membrane vesicles, MΦ-NPs, and NT[PA] as measured by dynamic light scattering ( $n = 3$ , mean + SD). (f) Representative transmission electron microscopy image of negatively stained NT[PA] (scale bar = 100 nm). (g) Size of NT[PA] over 7 weeks when stored in 10% sucrose at 4 °C ( $n = 3$ , mean  $\pm$  SD). No significant differences between day 0 and any other time point; one-way ANOVA.

formulation.<sup>32,36–39</sup> Because of their efficient lymphatic transport and ability to deliver antigens in their native form,

nanovaccines based on cell membrane coating technology can efficiently elicit disease-specific immune responses.<sup>30,31</sup> In

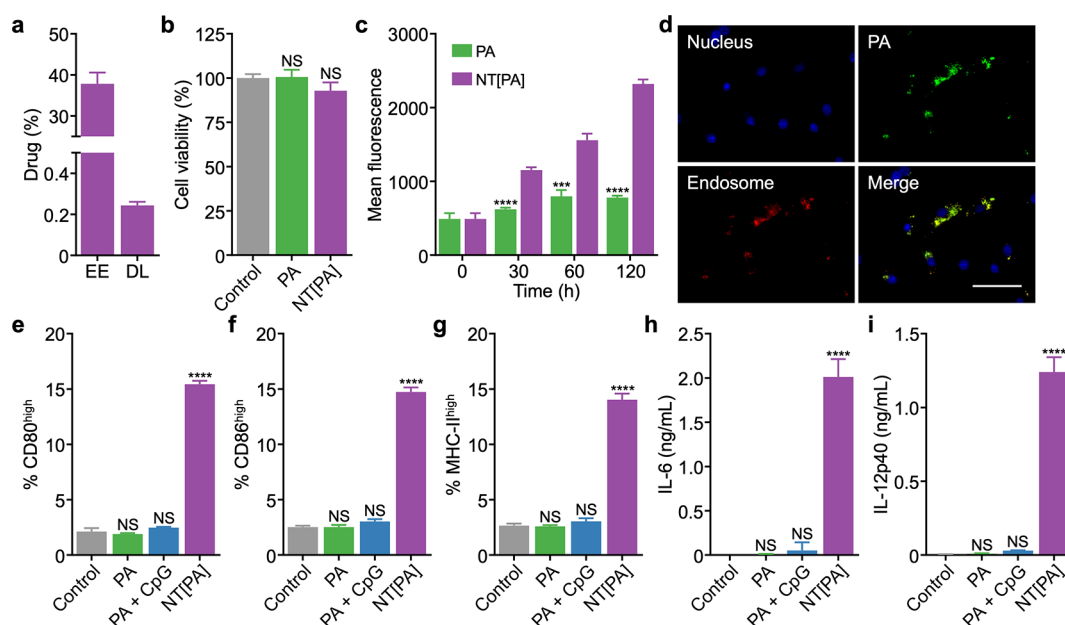


**Figure 3.** *In vitro* safety, uptake, and immune simulation. (a) Encapsulation efficiency (EE) and drug loading yield (DL) of CpG into NT[PA] ( $n = 3$ , mean + SD). (b) Viability of BMDCs after overnight incubation with free PA or NT[PA] ( $n = 3$ , mean + SD). NS = not significant (compared to control); one-way ANOVA. (c) BMDC uptake of dye-labeled PA in free form or on NT[PA] as analyzed by flow cytometry ( $n = 3$ , mean + SD). \*\*\* $p < 0.001$ , \*\*\*\* $p < 0.0001$ ; Student's  $t$ -test. (d) Representative fluorescent microscopy images of BMDCs after 30 min of incubation with NT[PA] (blue: nuclei [DAPI], green: PA [FITC], red: endosomes [LysoTracker]; scale bar = 50  $\mu\text{m}$ ). (e–g) Expression of maturation markers CD80 (e), CD86 (f), and MHC-II (g) on CD11c<sup>+</sup> BMDCs after pulsing with free PA only, free PA with CpG, or NT[PA] ( $n = 3$ , mean + SD). \*\*\*\* $p < 0.0001$ , NS = not significant (compared to control); one-way ANOVA. (h, i) Secretion of proinflammatory cytokines IL-6 (h) and IL-12p40 (i) by BMDCs after pulsing with free PA only, free PA with CpG, or NT[PA] ( $n = 3$ , mean + SD). \*\*\*\* $p < 0.0001$ , NS = not significant (compared to control); one-way ANOVA.

addition, by introducing an additional payload into the nanoparticle core, this platform enables codelivery of antigen and adjuvant, significantly improving the stimulation of immune cells.<sup>40,41</sup> Inspired by the natural interaction between PA and macrophages during *B. anthracis* infections, we fabricated a PA-bound nanotoxoid (NT[PA]) using an adjuvant-loaded macrophage membrane-coated nanoparticle (Figure 1). After a single, low-dose vaccination using NT[PA], the nanovaccine elicited strong and long-lasting immunity that protected mice against subsequent challenge with anthrax toxins.

## RESULTS AND DISCUSSION

**Fabrication and Characterization of NT[PA].** To fabricate a biomimetic nanoparticulate substrate capable of efficiently complexing with PA, the membrane from murine J774 macrophages was purified and coated onto self-assembled poly(lactic-co-glycolic acid) (PLGA) cores to yield macrophage membrane-coated nanoparticles (M $\Phi$ -NPs). J774 cells were chosen based on their established CMG2 expression,<sup>42</sup> and Western blotting was used to verify that the receptor for anthrax PA was retained throughout the M $\Phi$ -NP fabrication process (Figure 2a). Next, the nanoparticle solution was adjusted to pH 5.6 and 1 mM Mg<sup>2+</sup>, which helped to facilitate proper binding with PA after 30 min of coincubation.<sup>43,44</sup> The resulting NT[PA] was purified via centrifugation. The loading efficiency of PA onto the nanotoxoids was evaluated at varying J774 membrane protein to PA antigen weight ratios using a fluorescently labeled version of PA (Figure 2b). Loading saturation was observed at ratios above 100:1, which was chosen to fabricate NT[PA] for subsequent studies. PA loading was also confirmed by Western blotting analysis, which

revealed the strong presence of the anthrax antigen on NT[PA], but not on M $\Phi$ -NPs (Figure 2c). Dynamic light scattering (DLS) showed that after PA complexation the size of NT[PA] was comparable to that of M $\Phi$ -NPs (Figure 2d), and the zeta potential remained unchanged (Figure 2e). A clear core–shell structure was observed when viewing the nanoparticles under transmission electron microscopy (TEM) images with negative staining, further confirming successful membrane coating (Figure 2f). In addition, the final NT[PA] formulation demonstrated excellent stability, retaining its size in solution for up to 7 weeks when stored at 4 °C (Figure 2g). Quantitative Western blot analysis revealed that the PA remained strongly associated with the nanoparticles even after 24 h of incubation in biological buffer, further supporting the stability of NT[PA] (Figure S1).

**Adjuvant Loading, Safety, and Uptake.** To further enhance the potency of the nanotoxoid vaccine, CpG 1826, a nucleic acid-based adjuvant that is an agonist for Toll-like receptor 9 (TLR9),<sup>45</sup> was encapsulated into the polymeric core through a double emulsion fabrication technique.<sup>41</sup> The encapsulation efficiency was approximately 40%, resulting in a loading of 2.4  $\mu\text{g}$  of CpG per 1 mg of PLGA (Figure 3a). The prolonged release of CpG and other oligonucleotides from PLGA nanoparticle cores, including those coated with cell membrane, has been previously established.<sup>46–48</sup> All subsequent studies were conducted using NT[PA] fabricated with a CpG-loaded PLGA core. Next, the safety of NT[PA] was evaluated *in vitro* using bone marrow-derived dendritic cells (BMDCs) (Figure 3b). Given that PA itself is not cytotoxic in the absence of anthrax LF or edema factor (EF),<sup>49</sup> it was unsurprising that NT[PA] also did not display any toxicity at an equivalent antigen dose. Because of the fact that

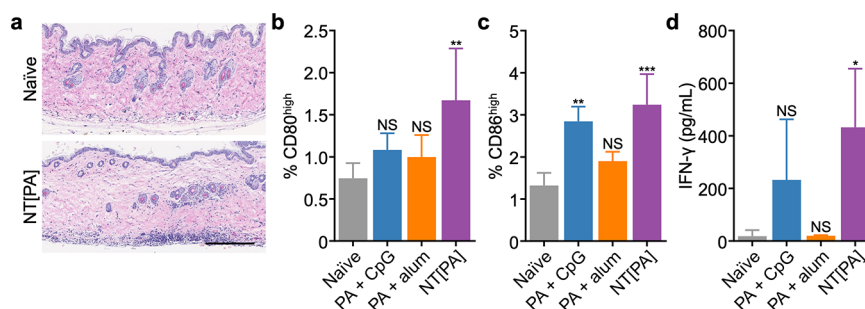


**Figure 4.** *In vivo* immune stimulation. (a) Representative histological sections of skin samples collected from naive mice or mice 24 h after subcutaneous injection with NT[PA] (scale bar = 250  $\mu$ m). (b, c) Expression of maturation markers CD80 (b) and CD86 (c) by CD11c<sup>+</sup> dendritic cells in the draining lymph nodes after subcutaneous administration of free PA with CpG, free PA with alum, or NT[PA] ( $n = 4$ , mean  $\pm$  SD). (d) Secretion of IFN- $\gamma$  by splenocytes pulsed *ex vivo* with PA for 7 days; the splenocytes were derived from mice 10 days after vaccination using free PA with CpG, free PA with alum, or NT[PA] ( $n = 3$ , mean  $\pm$  SD). \* $p < 0.05$ , \*\* $p < 0.01$ , \*\*\* $p < 0.001$ , NS = not significant (compared to naive); one-way ANOVA.

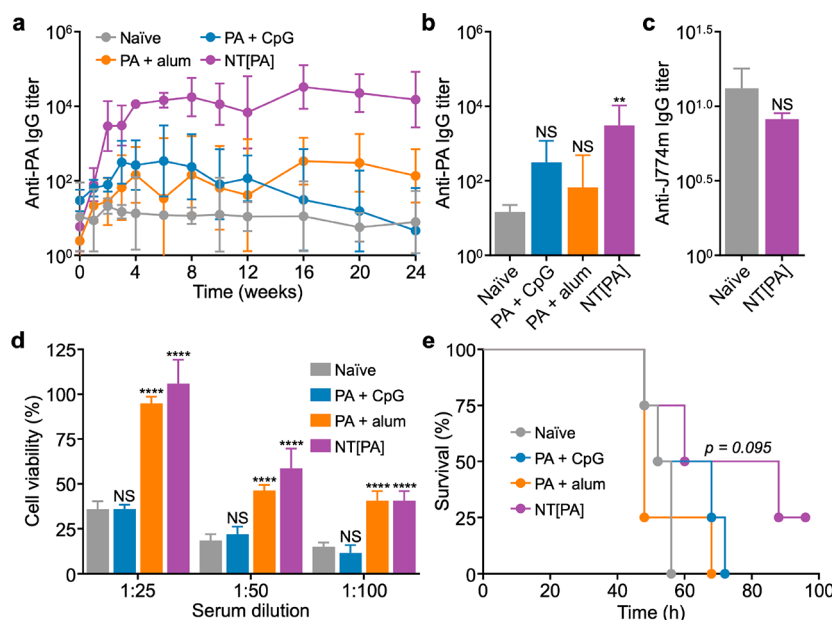


**Figure 5.** Antibody titers and protective efficacy. (a, b) Anti-PA IgG titers over time (a) or on day 21 (b) in the serum of mice following a single vaccination using free PA with CpG, free PA with alum, or NT[PA] ( $n = 3$ , mean  $\pm$  SD). \*\* $p < 0.01$ , NS = not significant (compared to naive); one-way ANOVA. (c) Anti-J774 membrane (anti-J774m) IgG titers in the serum of mice on day 28 after vaccination using NT[PA] ( $n = 3$ , mean  $\pm$  SD). NS = not significant; Student's  $t$ -test. (d) Viability of J774 cells 24 h after the addition of anthrax lethal toxin preincubated with various amounts of immune sera collected from mice 28 days after vaccination using free PA with CpG, free PA with alum, or NT[PA] ( $n = 9$ , mean  $\pm$  SD). \*\*\*\* $p < 0.0001$ , NS = not significant (compared to naive); one-way ANOVA. (e) Survival of mice challenged with anthrax lethal toxin 21 days after vaccination using free PA with CpG, free PA with alum, and NT[PA] ( $n = 4$ ).  $p$ -value compared to naive; log-rank test.

nanoparticles are readily internalized by antigen-presenting cells,<sup>41</sup> it was observed that PA was taken up more rapidly and to a higher degree by BMDCs when incorporated into NT[PA] rather than in free form (Figure 3c). Additionally, when delivered via the nanotoxoid formulation for 30 min, PA began localizing at varying degrees to the endosomes (Figure 3d), which suggested favorable CpG engagement with endosomal TLR9.<sup>50</sup>

**In Vitro Dendritic Cell Maturation.** To confirm the biological activity of the encapsulated CpG payload, NT[PA] and various control samples were first incubated with BMDCs *in vitro*. When evaluating the maturation markers CD80 and CD86 as well as major histocompatibility complex II (MHC-II), it was observed that BMDCs pulsed with NT[PA] had the highest expression (Figure 3e–g). In contrast, equivalent amounts of free PA with or without free CpG were unable to

induce significant BMDC maturation, likely due to their inefficient cellular uptake and inability to engage with TLR9 in the endosomes.<sup>41</sup> Similar trends were observed when analyzing secretion of the proinflammatory cytokines interleukin (IL)-6 and IL-12p40, with NT[PA] significantly outperforming the controls (Figure 3h,i). Overall, the data highlighted the importance of nanoparticulate delivery, which significantly boosted the activity of CpG for stimulating antigen-presenting cells.

**In Vivo Immune Activation.** Encouraged by the safety and activity of NT[PA] *in vitro*, we next evaluated the effect of the formulation when administered *in vivo* into mice. First, NT[PA] was injected subcutaneously, and skin samples were collected after 24 h for histological analysis (Figure 4a). A moderately higher level of inflammatory infiltrate appeared in the dermis of vaccinated mice when compared to naive mice,



which could be attributed to the immunostimulatory nature of NT[PA]. Otherwise, the epidermis remained intact after administration of the NT[PA] nanovaccine, suggesting a favorable safety profile. Next, we aimed to evaluate *in vivo* dendritic cell maturation in response to vaccination. Mice were subcutaneously administered with NT[PA], free PA mixed with CpG, or PA adsorbed to alum as a clinically relevant adjuvant.<sup>11</sup> The draining lymph nodes were collected after 48 h to analyze maturation markers by flow cytometry (Figure 4b,c). Compared to free PA with CpG or free PA mixed with alum, NT[PA] was the most efficient at upregulating expression of the maturation markers CD80 and CD86 on dendritic cells. In addition to the stimulation of antigen-presenting cells, T cell activation has been identified as critical for achieving complete protection against anthrax.<sup>51–54</sup> Antigen-specific cellular immunity was thus evaluated *ex vivo* using splenocytes that were harvested from mice 10 days after vaccination. After 7 days of restimulation by coculturing with PA, only the splenocytes from mice that received NT[PA] produced levels of interferon  $\gamma$  (IFN- $\gamma$ ) that were significantly elevated (Figure 4d). Notably, the splenocytes from mice receiving PA adjuvanted with alum were unable to produce any IFN- $\gamma$ , consistent with the fact that alum is ineffective at eliciting T helper 1 (Th1)-biased immunity.<sup>55</sup>

**Antibody Production and Protective Efficacy.** It is well established that neutralizing antibodies are the cornerstone of protective immunity against anthrax.<sup>56</sup> To evaluate antibody generation, mice were subcutaneously vaccinated with various formulations at a low antigen dose of 50 ng. The serum was then collected periodically and monitored for antibodies against PA (Figure 5a,b). The titers for mice vaccinated with NT[PA] elevated rapidly in the first 2 weeks and saturated at approximately 4 weeks, after which they persisted at the same level for a minimum of 24 weeks. While antigen-specific antibody production after vaccination using free PA with either CpG or alum appeared to trend upward in the first few weeks, anti-PA titer levels were inconsistent over time and lower in magnitude. The ability of the generated titers to bind PA was confirmed by Western blotting analysis using serum samples as the primary probe (Figure S2). To further dissect the immune response to NT[PA] vaccination, IgG subclassing was performed (Figure S3). Both IgG1 and IgG2 subtypes were highly present, suggesting balanced immunity along the Th1/Th2 axis.<sup>55</sup> To study the potential risk for generating autoimmunity, we evaluated the production of antibodies against J774 macrophage membrane and found that there was no significant elevation of titer levels over baseline (Figure 5c).

It is vital that the anti-PA antibodies generated from NT[PA] vaccination can neutralize the activity of anthrax toxins. As such, we evaluated the ability of immune sera from vaccinated mice to protect J774 cells from lethal toxin *in vitro* (Figure 5d). There was a clear dose-dependent neutralization effect when employing serum samples collected from mice vaccinated with NT[PA]. Sera from mice receiving free PA adjuvanted with alum also exhibited neutralizing activity, whereas the samples from mice vaccinated with free PA and CpG had minimal effects on cell viability. Finally, to assess if the enhanced immunity afforded by NT[PA] vaccination would translate into enhanced protection against anthrax *in vivo*, vaccinated mice were challenged with a high bolus dose of lethal toxin (Figure 5e). Mice in the NT[PA] group exhibited a median survival that was 20 h longer than that of naïve mice, with the difference between the two groups approaching

significance ( $p = 0.095$ ). In contrast, mice vaccinated using soluble PA with CpG or alum as an adjuvant had considerably shorter median survival times. Overall, the data suggested that the codelivery of PA together with an adjuvant in nanoparticulate form was critical for maximizing protection against anthrax lethal toxin.

## CONCLUSION

In conclusion, we have developed a biomimetic nanovaccine capable of safely and effectively generating protective immunity against anthrax toxins. By taking advantage of the natural cellular tropism of PA, a major *B. anthracis* virulence factor, we generated a nanotoxoid formulation by utilizing a macrophage membrane-coated nanoparticle encapsulated with a potent immunological adjuvant. The nanoparticles were able to complex with PA upon coincubation, thus enabling the resulting formulation to effectively codeliver both antigen and adjuvant to antigen-presenting cells. When administered to mice, a single low dose of the nanotoxoids elicited strong humoral and cellular immunity, outperforming free PA delivered with CpG or the clinically relevant alum as an adjuvant. Future studies can be conducted to optimize the dosing regimen and evaluate the potential benefit of booster vaccinations. Optimization of the membrane coating source, including the use of genetically engineered cell membranes,<sup>57–59</sup> could increase the antigen loading capacity of the nanotoxoids. Overall, this platform demonstrates the versatility of biomimetic nanotechnology, which enables the streamlined development of novel vaccine formulations capable of strongly activating immune responses for protection against infectious diseases.

## ASSOCIATED CONTENT

### Supporting Information

The Supporting Information is available free of charge at <https://pubs.acs.org/doi/10.1021/acs.nanolett.2c03881>.

Detailed information about materials and methods; PA binding stability (Figure S1); antibody binding to PA (Figure S2); anti-PA IgG subclassing (Figure S3) (PDF)

## AUTHOR INFORMATION

### Corresponding Authors

Ronnie H. Fang – Department of NanoEngineering, Chemical Engineering Program, and Moores Cancer Center, University of California, San Diego, La Jolla, California 92093, United States; [orcid.org/0000-0001-6373-3189](https://orcid.org/0000-0001-6373-3189); Email: [rhfang@ucsd.edu](mailto:rhfang@ucsd.edu)

Liangfang Zhang – Department of NanoEngineering, Chemical Engineering Program, and Moores Cancer Center, University of California, San Diego, La Jolla, California 92093, United States; [orcid.org/0000-0003-0637-0654](https://orcid.org/0000-0003-0637-0654); Email: [zhang@ucsd.edu](mailto:zhang@ucsd.edu)

### Authors

Maya Holay – Department of NanoEngineering, Chemical Engineering Program, and Moores Cancer Center, University of California, San Diego, La Jolla, California 92093, United States

Nishta Krishnan – Department of NanoEngineering, Chemical Engineering Program, and Moores Cancer Center, University of California, San Diego, La Jolla, California 92093, United States

Jiarong Zhou – Department of NanoEngineering, Chemical Engineering Program, and Moores Cancer Center, University of California, San Diego, La Jolla, California 92093, United States

Yaou Duan – Department of NanoEngineering, Chemical Engineering Program, and Moores Cancer Center, University of California, San Diego, La Jolla, California 92093, United States

Zhongyuan Guo – Department of NanoEngineering, Chemical Engineering Program, and Moores Cancer Center, University of California, San Diego, La Jolla, California 92093, United States

Weimei Gao – Department of NanoEngineering, Chemical Engineering Program, and Moores Cancer Center, University of California, San Diego, La Jolla, California 92093, United States; [orcid.org/0000-0001-5196-4887](https://orcid.org/0000-0001-5196-4887)

Complete contact information is available at:

<https://pubs.acs.org/10.1021/acs.nanolett.2c03881>

## Notes

The authors declare no competing financial interest.

## ACKNOWLEDGMENTS

This work was supported by the Defense Threat Reduction Agency Joint Science and Technology Office for Chemical and Biological Defense under Grants HDTRA1-18-1-0014 and HDTRA1-21-1-0010 and the National Institutes of Health under Award R21AI159492.

## REFERENCES

- (1) Carlson, C. J.; Krcalik, I. T.; Ross, N.; Alexander, K. A.; Hugh-Jones, M. E.; Fegan, M.; Elkin, B. T.; Epp, T.; Shury, T. K.; Zhang, W.; Bagirova, M.; Getz, W. M.; Blackburn, J. K. The Global Distribution of *Bacillus anthracis* and Associated Anthrax Risk to Humans, Livestock and Wildlife. *Nat. Microbiol.* **2019**, *4*, 1337–1343.
- (2) Sternbach, G. The History of Anthrax. *J. Emerg. Med.* **2003**, *24*, 463–467.
- (3) Moayeri, M.; Leppla, S. H.; Vrentas, C.; Pomerantsev, A. P.; Liu, S. Anthrax Pathogenesis. *Annu. Rev. Microbiol.* **2015**, *69*, 185–208.
- (4) Manish, M.; Verma, S.; Kandari, D.; Kulshreshtha, P.; Singh, S.; Bhatnagar, R. Anthrax Prevention Through Vaccine and Post-Exposure Therapy. *Expert Opin. Biol. Ther.* **2020**, *20*, 1405–1425.
- (5) Brookmeyer, R.; Johnson, E.; Bollinger, R. Modeling the Optimum Duration of Antibiotic Prophylaxis in an Anthrax Outbreak. *Proc. Natl. Acad. Sci. U. S. A.* **2003**, *100*, 10129–10132.
- (6) Chen, Z.; Moayeri, M.; Purcell, R. Monoclonal Antibody Therapies against Anthrax. *Toxins* **2011**, *3*, 1004–1019.
- (7) Liu, S.; Moayeri, M.; Leppla, S. H. Anthrax Lethal and Edema Toxins in Anthrax Pathogenesis. *Trends Microbiol.* **2014**, *22*, 317–325.
- (8) Liu, S.; Miller-Randolph, S.; Crown, D.; Moayeri, M.; Sastalla, I.; Okugawa, S.; Leppla, S. H. Anthrax Toxin Targeting of Myeloid Cells Through the CMG2 Receptor Is Essential for Establishment of *Bacillus anthracis* Infections in Mice. *Cell Host Microbe* **2010**, *8*, 455–462.
- (9) Romanenko, Y. O.; Riabko, A. K.; Marin, M. A.; Kartseva, A. S.; Silkina, M. V.; Shemyakin, I. G.; Firstova, V. V. Mechanism of Action of Monoclonal Antibodies That Block the Activity of the Lethal Toxin of *Bacillus anthracis*. *Acta Naturae* **2021**, *13*, 98–104.
- (10) Collier, R. J.; Young, J. A. Anthrax Toxin. *Annu. Rev. Cell Dev. Biol.* **2003**, *19*, 45–70.
- (11) Longstreth, J.; Skiadopoulos, M. H.; Hopkins, R. J. Licensure Strategy for Pre- and Post-Exposure Prophylaxis of Biothrax Vaccine: The First Vaccine Licensed Using the FDA Animal Rule. *Expert Rev. Vaccines* **2016**, *15*, 1467–1479.
- (12) Baylor, N. W.; Egan, W.; Richman, P. Aluminum Salts in Vaccines—US Perspective. *Vaccine* **2002**, *20*, S18–S23.
- (13) D'Souza, A. J.; Mar, K. D.; Huang, J.; Majumdar, S.; Ford, B. M.; Dyas, B.; Ulrich, R. G.; Sullivan, V. J. Rapid Deamidation of Recombinant Protective Antigen When Adsorbed on Aluminum Hydroxide Gel Correlates with Reduced Potency of Vaccine. *J. Pharm. Sci.* **2013**, *102*, 454–461.
- (14) Verma, A.; Burns, D. L. Improving the Stability of Recombinant Anthrax Protective Antigen Vaccine. *Vaccine* **2018**, *36*, 6379–6382.
- (15) Rynkiewicz, D.; Rathkopf, M.; Sim, I.; Waytes, A. T.; Hopkins, R. J.; Giri, L.; DeMuria, D.; Ransom, J.; Quinn, J.; Nabors, G. S.; Nielsen, C. J. Marked Enhancement of the Immune Response to BioThrax® (Anthrax Vaccine Adsorbed) by the TLR9 Agonist CPG 7909 in Healthy Volunteers. *Vaccine* **2011**, *29*, 6313–6320.
- (16) Klinman, D. M.; Xie, H.; Ivins, B. E. CpG Oligonucleotides Improve the Protective Immune Response Induced by the Licensed Anthrax Vaccine. *Ann. N. Y. Acad. Sci.* **2006**, *1082*, 137–150.
- (17) Klinman, D. M. CpG Oligonucleotides Accelerate and Boost the Immune Response Elicited by AVA, the Licensed Anthrax Vaccine. *Expert Rev. Vaccines.* **2006**, *5*, 365–369.
- (18) Tsai, M. H.; Chuang, C. C.; Chen, C. C.; Yen, H. J.; Cheng, K. M.; Chen, X. A.; Shyu, H. F.; Lee, C. Y.; Young, J. J.; Kau, J. H. Nanoparticles Assembled from Fucoidan and Trimethylchitosan as Anthrax Vaccine Adjuvant: In Vitro and In Vivo Efficacy in Comparison to CpG. *Carbohydr. Polym.* **2020**, *236*, 116041.
- (19) Malik, A.; Gupta, M.; Mani, R.; Gogoi, H.; Bhatnagar, R. Trimethyl Chitosan Nanoparticles Encapsulated Protective Antigen Protects the Mice against Anthrax. *Front. Immunol.* **2018**, *9*, 562.
- (20) Fang, R. H.; Kroll, A. V.; Gao, W.; Zhang, L. Cell Membrane Coating Nanotechnology. *Adv. Mater.* **2018**, *30*, 1706759.
- (21) Fang, R. H.; Jiang, Y.; Fang, J. C.; Zhang, L. Cell Membrane-Derived Nanomaterials for Biomedical Applications. *Biomaterials* **2017**, *128*, 69–83.
- (22) Hu, C. M.; Fang, R. H.; Wang, K. C.; Luk, B. T.; Thamphiwatana, S.; Dehaini, D.; Nguyen, P.; Angsantikul, P.; Wen, C. H.; Kroll, A. V.; Carpenter, C.; Ramesh, M.; Qu, V.; Patel, S. H.; Zhu, J.; Shi, W.; Hofman, F. M.; Chen, T. C.; Gao, W.; Zhang, K.; et al. Nanoparticle Biointerfacing by Platelet Membrane Cloaking. *Nature* **2015**, *526*, 118–121.
- (23) Fang, R. H.; Hu, C. M.; Luk, B. T.; Gao, W.; Copp, J. A.; Tai, Y.; O'Connor, D. E.; Zhang, L. Cancer Cell Membrane-Coated Nanoparticles for Anticancer Vaccination and Drug Delivery. *Nano Lett.* **2014**, *14*, 2181–2188.
- (24) Gao, W.; Fang, R. H.; Thamphiwatana, S.; Luk, B. T.; Li, J.; Angsantikul, P.; Zhang, Q.; Hu, C. M.; Zhang, L. Modulating Antibacterial Immunity via Bacterial Membrane-Coated Nanoparticles. *Nano Lett.* **2015**, *15*, 1403–1409.
- (25) Park, J. H.; Dehaini, D.; Zhou, J.; Holay, M.; Fang, R. H.; Zhang, L. Biomimetic Nanoparticle Technology for Cardiovascular Disease Detection and Treatment. *Nanoscale Horiz* **2020**, *5*, 25–42.
- (26) Zhuang, J.; Holay, M.; Park, J. H.; Fang, R. H.; Zhang, J.; Zhang, L. Nanoparticle Delivery of Immunostimulatory Agents for Cancer Immunotherapy. *Theranostics* **2019**, *9*, 7826–7848.
- (27) Fang, R. H.; Gao, W.; Zhang, L. Targeting Drugs to Tumours using Cell Membrane-Coated Nanoparticles. *Nat. Rev. Clin. Oncol.* **2022**, DOI: 10.1038/s41571-022-00699-x.
- (28) Wang, S.; Wang, D.; Duan, Y.; Zhou, Z.; Gao, W.; Zhang, L. Cellular Nanosponges for Biological Neutralization. *Adv. Mater.* **2022**, *34*, No. e2107719.
- (29) Fang, R. H.; Luk, B. T.; Hu, C. M.; Zhang, L. Engineered Nanoparticles Mimicking Cell Membranes for Toxin Neutralization. *Adv. Drug Delivery Rev.* **2015**, *90*, 69–80.
- (30) Kroll, A. V.; Jiang, Y.; Zhou, J.; Holay, M.; Fang, R. H.; Zhang, L. Biomimetic Nanoparticle Vaccines for Cancer Therapy. *Adv. Biosyst.* **2019**, *3*, 1800219.
- (31) Zhou, J.; Kroll, A. V.; Holay, M.; Fang, R. H.; Zhang, L. Biomimetic Nanotechnology toward Personalized Vaccines. *Adv. Mater.* **2020**, *32*, 1901255.

- (32) Guo, Z.; Kubiawicz, L. J.; Fang, R. H.; Zhang, L. Nanotoxoids: Biomimetic Nanoparticle Vaccines against Infections. *Adv. Ther.* **2021**, *4*, 2100072.
- (33) Hu, C. M.; Fang, R. H.; Copp, J.; Luk, B. T.; Zhang, L. A Biomimetic Nanosponge That Absorbs Pore-Forming Toxins. *Nat. Nanotechnol.* **2013**, *8*, 336–340.
- (34) Zhang, Q.; Dehaini, D.; Zhang, Y.; Zhou, J.; Chen, X.; Zhang, L.; Fang, R. H.; Gao, W.; Zhang, L. Neutrophil Membrane-Coated Nanoparticles Inhibit Synovial Inflammation and Alleviate Joint Damage in Inflammatory Arthritis. *Nat. Nanotechnol.* **2018**, *13*, 1182–1190.
- (35) Zhang, Q.; Honko, A.; Zhou, J.; Gong, H.; Downs, S. N.; Vasquez, J. H.; Fang, R. H.; Gao, W.; Griffiths, A.; Zhang, L. Cellular Nanosponges Inhibit SARS-CoV-2 Infectivity. *Nano Lett.* **2020**, *20*, 5570–5574.
- (36) Hu, C.-M. J.; Fang, R. H.; Luk, B. T.; Zhang, L. Nanoparticle-Detained Toxins for Safe and Effective Vaccination. *Nat. Nanotechnol.* **2013**, *8*, 933–938.
- (37) Wei, X.; Beltran-Gastelum, M.; Karshalev, E.; Esteban-Fernandez de Avila, B.; Zhou, J.; Ran, D.; Angsantikul, P.; Fang, R. H.; Wang, J.; Zhang, L. Biomimetic Micromotor Enables Active Delivery of Antigens for Oral Vaccination. *Nano Lett.* **2019**, *19*, 1914–1921.
- (38) Wei, X.; Ran, D.; Campeau, A.; Xiao, C.; Zhou, J.; Dehaini, D.; Jiang, Y.; Kroll, A. V.; Zhang, Q.; Gao, W.; Gonzalez, D. J.; Fang, R. H.; Zhang, L. Multiantigenic Nanotoxoids for Antivirulence Vaccination against Antibiotic-Resistant Gram-Negative Bacteria. *Nano Lett.* **2019**, *19*, 4760–4769.
- (39) Zhou, J.; Ventura, C. J.; Yu, Y.; Gao, W.; Fang, R. H.; Zhang, L. Biomimetic Neutrophil Nanotoxoids Elicit Potent Immunity against *Acinetobacter baumannii* in Multiple Models of Infection. *Nano Lett.* **2022**, *22*, 7057–7065.
- (40) Zhou, J.; Miyamoto, Y.; Ihara, S.; Kroll, A. V.; Nieskens, N.; Tran, V. N.; Hanson, E. M.; Fang, R. H.; Zhang, L.; Eckmann, L. Codelivery of Antigens and Adjuvant in Polymeric Nanoparticles Coated with Native Parasite Membranes Induces Protective Mucosal Immunity against *Giardia lamblia*. *J. Infect. Dis.* **2022**, *226*, 319–323.
- (41) Kroll, A. V.; Fang, R. H.; Jiang, Y.; Zhou, J.; Wei, X.; Yu, C. L.; Gao, J.; Luk, B. T.; Dehaini, D.; Gao, W.; Zhang, L. Nanoparticulate Delivery of Cancer Cell Membrane Elicits Multiantigenic Antitumor Immunity. *Adv. Mater.* **2017**, *29*, 1703969.
- (42) Male, A. L.; Forafonov, F.; Cuda, F.; Zhang, G.; Zheng, S.; Oyston, P. C. F.; Chen, P. R.; Williamson, E. D.; Tavassoli, A. Targeting *Bacillus anthracis* Toxicity with a Genetically Selected Inhibitor of the PA/CMG2 Protein-Protein Interaction. *Sci. Rep.* **2017**, *7*, 3104.
- (43) Petosa, C.; Collier, R. J.; Klimpel, K. R.; Leppla, S. H.; Liddington, R. C. Crystal Structure of the Anthrax Toxin Protective Antigen. *Nature* **1997**, *385*, 833–838.
- (44) Wigelsworth, D. J.; Krantz, B. A.; Christensen, K. A.; Lacy, D. B.; Juris, S. J.; Collier, R. J. Binding Stoichiometry and Kinetics of the Interaction of a Human Anthrax Toxin Receptor, CMG2, with Protective Antigen. *J. Biol. Chem.* **2004**, *279*, 23349–23356.
- (45) Klinman, D. M. Immunotherapeutic Uses of CpG Oligodeoxynucleotides. *Nat. Rev. Immunol.* **2004**, *4*, 249–259.
- (46) Xu, C.; Liu, W.; Hu, Y.; Li, W.; Di, W. Bioinspired Tumor-Homing Nanoplatform for Co-Delivery of Paclitaxel and siRNA-E7 to HPV-Related Cervical Malignancies for Synergistic Therapy. *Theranostics* **2020**, *10*, 3325–3339.
- (47) Ma, J.; Liu, F.; Sheu, W. C.; Meng, Z.; Xie, Y.; Xu, H.; Li, M.; Chen, A. T.; Liu, J.; Bao, Y.; Zhang, X.; Zhang, S.; Zhang, L.; Zou, Z.; Wu, H.; Wang, H.; Zhu, Y.; Zhou, J. Copresentation of Tumor Antigens and Costimulatory Molecules via Biomimetic Nanoparticles for Effective Cancer Immunotherapy. *Nano Lett.* **2020**, *20*, 4084–4094.
- (48) Lin, S. Y.; Yao, B. Y.; Hu, C. J.; Chen, H. W. Induction of Robust Immune Responses by CpG-ODN-Loaded Hollow Polymeric Nanoparticles for Antiviral and Vaccine Applications in Chickens. *Int. J. Nanomedicine* **2020**, *15*, 3303–3318.
- (49) Young, J. A.; Collier, R. J. Anthrax Toxin: Receptor Binding, Internalization, Pore Formation, and Translocation. *Annu. Rev. Biochem.* **2007**, *76*, 243–265.
- (50) Chaturvedi, A.; Pierce, S. K. How Location Governs Toll-Like Receptor Signaling. *Traffic* **2009**, *10*, 621–628.
- (51) Glomski, I. J.; Corre, J. P.; Mock, M.; Goossens, P. L. Cutting Edge: IFN- $\gamma$ -Producing CD4 T Lymphocytes Mediate Spore-Induced Immunity to Capsulated *Bacillus anthracis*. *J. Immunol.* **2007**, *178*, 2646–2650.
- (52) Ingram, R. J.; Metan, G.; Maillere, B.; Doganay, M.; Ozkul, Y.; Kim, L. U.; Baillie, L.; Dyson, H.; Williamson, E. D.; Chu, K. K.; Ascough, S.; Moore, S.; Huwar, T. B.; Robinson, J. H.; Srisikandan, S.; Altmann, D. M. Natural Exposure to Cutaneous Anthrax Gives Long-Lasting T Cell Immunity Encompassing Infection-Specific Epitopes. *J. Immunol.* **2010**, *184*, 3814–3821.
- (53) Quinn, C. P.; Sabourin, C. L.; Niemuth, N. A.; Li, H.; Semenova, V. A.; Rudge, T. L.; Mayfield, H. J.; Schiffer, J.; Mittler, R. S.; Ibegbu, C. C.; Wrammert, J.; Ahmed, R.; Brys, A. M.; Hunt, R. E.; Levesque, D.; Estep, J. E.; Barnewall, R. E.; Robinson, D. M.; Plikaytis, B. D.; Marano, N.; et al. A Three-Dose Intramuscular Injection Schedule of Anthrax Vaccine Adsorbed Generates Sustained Humoral and Cellular Immune Responses to Protective Antigen and Provides Long-Term Protection Against Inhalation Anthrax in Rhesus Macaques. *Clin. Vaccine Immunol.* **2012**, *19*, 1730–1745.
- (54) Boyaka, P. N.; Tafaro, A.; Fischer, R.; Leppla, S. H.; Fujihashi, K.; McGhee, J. R. Effective Mucosal Immunity to Anthrax: Neutralizing Antibodies and Th Cell Responses Following Nasal Immunization with Protective Antigen. *J. Immunol.* **2003**, *170*, 5636–5643.
- (55) Weeratna, R. D.; Brazolot Millan, C. L.; McCluskie, M. J.; Davis, H. L. CpG ODN Can Re-Direct the Th Bias of Established Th2 Immune Responses in Adult and Young Mice. *FEMS Microbiol. Immunol.* **2001**, *32*, 65–71.
- (56) Reuveny, S.; White, M. D.; Adar, Y. Y.; Kafri, Y.; Altboum, Z.; Gozes, Y.; Kobiler, D.; Shafferman, A.; Velan, B. Search for Correlates of Protective Immunity Conferred by Anthrax Vaccine. *Infect. Immun.* **2001**, *69*, 2888–2893.
- (57) Jiang, Y.; Krishnan, N.; Zhou, J.; Chekuri, S.; Wei, X.; Kroll, A. V.; Yu, C. L.; Duan, Y.; Gao, W.; Fang, R. H.; Zhang, L. Engineered Cell-Membrane-Coated Nanoparticles Directly Present Tumor Antigens to Promote Anticancer Immunity. *Adv. Mater.* **2020**, *32*, 2001808.
- (58) Park, J. H.; Jiang, Y.; Zhou, J.; Gong, H.; Mohapatra, A.; Heo, J.; Gao, W.; Fang, R. H.; Zhang, L. Genetically Engineered Cell Membrane-Coated Nanoparticles for Targeted Delivery of Dexamethasone to Inflamed Lungs. *Sci. Adv.* **2021**, *7*, No. eabf7820.
- (59) Park, J. H.; Mohapatra, A.; Zhou, J.; Holay, M.; Krishnan, N.; Gao, W.; Fang, R. H.; Zhang, L. Virus-Mimicking Cell Membrane-Coated Nanoparticles for Cytosolic Delivery of mRNA. *Angew. Chem., Int. Ed. Engl.* **2022**, *61*, No. e202113671.